Carbohydrate Polymers 91 (2013) 183–190

Contents lists available at SciVerse ScienceDirect

Carbohydrate Polymers

journal homepage: www.elsevier.com/locate/carbpol

Network formation of nanofibrillated cellulose in solution blended poly(methyl methacrylate) composites

Kuisma Littunen, Ulla Hippi, Tapio Saarinen, Jukka Seppälä*

Polymer Technology, Department of Biotechnology and Chemical Technology, Aalto University School of Chemical Technology, P.O. Box 16100, 00076 Aalto, Finland

ARTICLE INFO

Article history:
Received 9 May 2012
Received in revised form 20 July 2012
Accepted 9 August 2012
Available online 18 August 2012

Keywords:
Nanofibrillated cellulose
PMMA
Nanocomposite
Percolation
Graft copolymerization

ABSTRACT

Composites of poly(methyl methacrylate) (PMMA) and nanofibrillated cellulose (NFC) were prepared by solution blending and further processed by injection and compression molding. To improve adhesion at the PMMA/NFC interface, the nanofibrils were covalently grafted with PMMA. Formation of a percolating nanofibril network was observed between 1 and 5 wt.% of NFC by dynamic rotational rheometry in molten state. This observation was further supported by the behavior of glass transition temperature which decreased at low NFC concentrations but recovered above the percolation threshold, indicating a decreased mobility of the matrix polymer. This effect was more pronounced with ungrafted NFC, possibly due to a stronger network. The unmodified NFC induced a minor degradation of the molar mass of PMMA. As thin plates, the composites were transparent at low NFC concentrations but became partially aggregated at the highest NFC concentrations. Despite the continuous NFC network, tensile testing showed no improvement of the mechanical properties.

1. Introduction

Nanofibrillated cellulose (NFC) is a wood-based nanomaterial, prepared from pulp by mainly mechanical grinding or fluidization, sometimes combined with chemical or enzymatic pretreatments. The fibrils are below 100 nm in diameter and up to several micrometers long. Their specific surface area is also very large due to the small diameter and large aspect ratio (Pääkkö et al., 2007; Turbak, Snyder, & Sandberg, 1983). NFC has attracted increasing attention during the past decade because of its many unique properties. Due to the low amount of structural defects, the mechanical strength of an individual nanofibril is far superior to a pulp fiber, approaching the properties of a perfect cellulose crystal. The high strength and expanded surface area make NFC a promising reinforcement material for polymer composites (Helbert, Cavaillé, & Dufresne, 1996). Another interesting feature of NFC is its tendency to form a continuous, web-like network of interconnected nanofibers in suspensions already at very low concentrations (Pääkkö et al., 2007). In polymer composites, the network can increase toughness by preventing crack propagation. Composites reinforced with NFC have exhibited significantly higher tensile strength and elongation at break, compared to corresponding pulp fiber composites (Nakagaito & Yano, 2005). The fibril diameter, being far below the wavelength of visible light, also enables the reinforcement of transparent polymers without compromising their optical properties. Moreover, the transparency of nanocomposites is highly insensitive to the refractive indices of the components and therefore also to temperature variations (Nogi, Handa, Nakagaito, & Yano, 2005).

The main challenges in composite applications are associated with the high hydrophilicity of cellulose, which makes it incompatible with many bulk polymers (Berglund, 2005). One approach to improve the adhesion in NFC composites is the grafting of synthetic polymers from the NFC surface. Covalently attached polymer layer increases adhesion between solid surfaces due to entanglements (Nordgren, Lonnberg, Hult, Malmstrom, & Rutland, 2009), suggesting that graft copolymerized cellulose also has stronger affinity to a surrounding polymer matrix. These copolymers are simple to synthesize by using several acrylic monomers (Littunen et al., 2011).

Poly(methyl methacrylate) (PMMA) is a glass-clear polymer which has many uses in optical applications. Its applicability is limited by the relatively low mechanical strength and susceptibility to scratching. To reinforce PMMA, it has been blended with natural and modified cellulose fibers by melt compounding. The grafting approach has been tested in order to improve the adhesion between the fibers and the polymer, by using cellulose fibers grafted with PMMA and poly(butyl acrylate) (PBA) (Canché-Escamilla et al., 2002). Addition of cellulose grafted with PMMA resulted in slightly higher elastic modulus, while the addition of PBA grafted cellulose made the composite less rigid and improved the impact strength notably. However, relatively high amounts of fiber were needed for these improvements, leading to deterioration of the tensile strength.

---

* Corresponding author. Tel.: +358 9 4702 2614; fax: +358 9 462 373.
E-mail address: jukka.seppala@aalto.fi (J. Seppälä).

0144-8617/$ – see front matter © 2012 Elsevier Ltd. All rights reserved.
http://dx.doi.org/10.1016/j.carbpol.2012.08.032

Melt blending is a very common method to make polymer composites but it has been found to be problematic in the preparation of cellulose nanocomposites because nano-sized cellulose forms strong aggregates during drying that are not properly redispersed during the melt processing. The other possibility is to feed NFC into extruder as a water suspension. In this case, there is a risk of foaming due to the evaporating water (Bondeson & Oksman, 2007). Moreover, the presence of water at high temperatures can be detrimental to polymers containing e.g. amide or ester bonds (Taubner & Shishoo, 2001). For these reasons, we wanted to investigate the possibility to mix NFC suspension with dissolved polymer, which allows efficient drying of NFC with less aggregation and enables also the mixing of the components before molding.

Solution blending has been studied by impregnating regenerated cellulose films with dissolved PMMA over a wide concentration range. A linear increase in modulus and tensile strength was observed with increasing cellulose content in PMMA composites, approaching the values of pure cellulose (Isobe, Sekine, Kimura, Wada, & Kuga, 2011).

Only few studies have been published on mixing nano-sized cellulose with PMMA. Cellulose nanocrystals (CNC) have been used in composites prepared by solution blending and subsequent casting into transparent sheets by evaporating the solvent (Liu, Liu, Yao, & Wu, 2010), and by electrospinning into sub-micron sized fibers (Dong et al., 2012). In both cases, the storage modulus was found to increase with the addition of CNC, but the effect on the tensile properties of PMMA was not determined.

In this paper, we report the preparation of PMMA/NFC composites by solution blending. By using cellulose nanofibers instead of nanocrystals, it was possible to study also the network-forming behavior of NFC. To investigate the possible contribution of the grafted polymer to the interfacial adhesion and network strength, both unmodified and PMMA-grafted NFC were used in the composites. The gel character of the materials in molten state was determined by dynamic rotational rheometry and the effect of NFC to the mobility of the polymer chains was studied by dynamic scanning calorimetry (DSC). Information about adhesion, transparency, and dispersion was collected by visible light transmittance measurements and mechanical testing of the composites.

2. Experimental

2.1. Materials

Nanofibrillated cellulose was provided by UPM Corporation (Helsinki, Finland) with a product name UPM Fibril Cellulose. The material was prepared by mechanical disintegration of bleached birch pulp, which was pre-treated with a Voith refiner and then fluidized by seven passes through an M7115 fluidizer (Microfluidics Corp, Newton, MA, USA). The solids content of the prepared water dispersion was 1.6 wt.%. Tetrahydrofuran (THF, analytical grade) was purchased from VWR (Karlskoga, Sweden) and PMMA (M_n = 70 kg/mol) from LG Chem (Seoul, South Korea).

2.2. Graft copolymerization

The grafting of NFC was carried out by free radical graft copolymerization with methyl methacrylate (MMA) in aqueous suspension. The method was described in detail in our earlier article, and the product used in this study was identical to the NFC-PMMA 4 batch reported therein (Littunen et al., 2011). The polymerization time was 60 min, 2 mmol/dm^3 of cerium (IV) ammonium nitrate (CAN) was used as initiator, and the amount of monomer was 40 mmol/g of dry NFC. Simultaneously formed homopolymer was removed from the product by washing with THF. The PMMA content of the grafted NFC, determined gravimetrically, was 49 wt.%. The grafted polymer was isolated by hydrolyzing the cellulose backbone with sulfuric acid and its molar mass was measured by gel permeation chromatography (GPC). The number average molar mass of the grafted PMMA was 127,000 g/mol, and its polydispersity index (PDI) was 1.88.

2.3. Solution blending

Commercial PMMA (10 g) was dissolved in THF as 15 wt.% solution, and never-dried NFC (neat or grafted) was centrifuged and redispersed twice in acetone and then three times in THF. The NFC suspension was poured into the PMMA solution to yield a concentration of 0.5, 1.0, 5.0 or 15 wt.% of dry cellulose. The mixture was agitated by a magnetic stirrer until no visible aggregates were observed, and dried at ambient temperature.

2.4. Preparation of the test specimens

Materials were dried at 60 °C overnight before molding. Plates of 0.5 mm in thickness were compression molded at 210 °C with a TP 400 plate press (Fontijne Grotnes BV, Vlaardingen, Netherlands) for evaluation of transparency and melt rheology. Tensile test bars were prepared with a mini-injection molding machine (DSM, Heerlen, Netherlands). The temperature of the injection cylinder and the mold were 230 and 100 °C, respectively.

Tensile properties were characterized with an Instron 4204 testing machine (Norwood, MA, USA) with a test speed of 2 mm/min. The specimen type was 1.5 mm thick 1BA according to the standard ISO 527-1993 (E).

2.5. Melt viscosity

The rheological data was recorded using Physica MCR 301 rotational rheometer (Anton Paar GmbH, Austria). The rheometer was equipped with CTD 450 convection heated oven and 25 mm parallel plates geometry, and measurements were conducted at 210 °C under nitrogen atmosphere.

The measurements consisted of frequency sweeps at angular frequencies (ω) from 628 to 0.1 rad/s with a strain of 0.5%, i.e. well within the linear viscoelastic region. The stability of the sample over the course of the measurement was verified by running a short time sweep measurement, $\omega = 1$ rad/s, strain 0.5%, prior and after the frequency sweep.

2.6. Thermal properties

In order to study the effect of NFC on the mobility of the polymer matrix, the glass transition temperatures (T_g) of the composites were determined. The analyses were performed on a Star DSC 821e equipment from Mettler-Toledo, Inc. (Columbus, OH, USA). Samples of the injection molded specimen were heated twice from 25 to 160 °C at a rate of 20 °C/min, and the T_g values were determined during the second heating period. The results were averaged from three samples of each composite to compensate the effect of possible inhomogeneity.

2.7. Optical properties

The appearance and homogeneity of the composite films were evaluated visually and the transparency was measured by spectrophotometry in the wavelength range of 400–700 nm with a Helios β UV/VIS spectrometer from Unicam, Inc. (UK). The results were averaged from three samples of each composite.

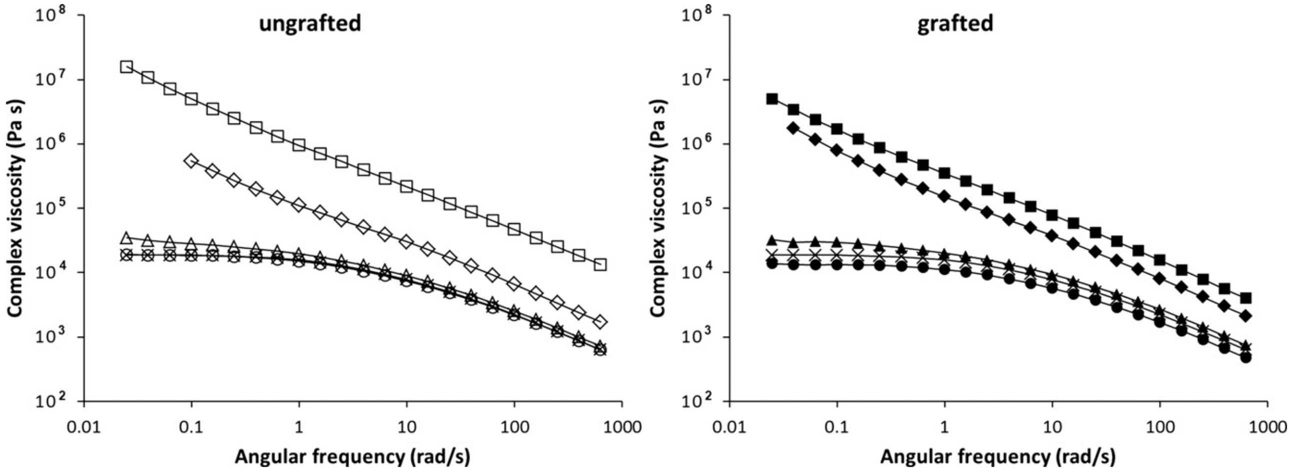

Fig. 1. Complex viscosities of PMMA (crosses) and composites with 0.5 wt.% (circles), 1 wt.% (triangles), 5 wt.% (tilted squares), and 15 wt.% (squares) of ungrafted (left) or grafted (right) NFC.

2.8. Microscopic imaging

The fine structure of the unmodified and grafted NFC was studied with atomic force microscopy (AFM). The samples were prepared from never-dried dispersions by spin-coating on SiO_2 surface and imaged in air, using tapping mode, with a Nanoscope IIIa Multimode scanning probe microscope from Digital Instruments Inc. (Santa Barbara, CA, USA). Silicon cantilevers (NSC15/AIBS) from MicroMasch (Tallinn, Estonia) were used.

The microstructure and dispersion of NFC in the composites were analyzed by field emission scanning electron microscope (FE-SEM). Samples were prepared from the injection molded specimen with 1 and 5 wt.% NFC by breaking the specimen in half after freezing with liquid nitrogen. The images were taken with a 6335 F FE-SEM from JEOL (Tokyo, JP), using 5.0 kV acceleration voltage.

2.9. Molar mass

Molar masses of the matrix polymer were measured in order to determine the possible degradation of the polymer matrix during processing. Samples were cut from the injection molded specimen and they were analyzed on a gel permeation chromatography (GPC) equipment including an HPLC pump and a refractive index detector manufactured by Waters, Inc. (Milford, MA, USA), and PLgel columns. Chloroform was used as an eluent, and the calibration curve was obtained with polystyrene standards.

3. Results and discussion

Composites of NFC and PMMA were prepared by solution blending with NFC loads of 0.5, 1, 5, and 15 wt.%. The composite specimens were successfully injection molded with up to 5 wt.% of NFC. At the highest NFC content, the material was too viscous to fill the mold. The materials were then characterized for molar mass and mechanical, thermal, and optical properties.

3.1. Melt viscosity

Rheology of the samples was studied by oscillating measurements, giving information about the viscoelastic properties of the composites in the molten state. Complex viscosities of the composite samples are displayed in Fig. 1.

The smallest amount (0.5 wt.%) of ungrafted NFC had no effect on PMMA melt rheology. The same amount of grafted NFC decreased the complex viscosity slightly. Further addition of both NFC types also increased the complex viscosity at every concentration. The most significant change occurred between 1 and 5 wt.% but otherwise the changes were modest. Especially the difference between 5 and 15 wt.% was smaller than expected.

This is likely due to pronounced aggregate formation distorting the observed results. Large, dense aggregates that span the gap between upper and lower plates exaggerate the observed, apparent complex viscosity. On the other hand, should the size of the aggregate be smaller, but the sample still heterogeneous, the observed complex viscosity reflects more the fiber poor matrix value. 15 wt.% fiber content is too high for an even fiber distribution and the rheological results are arbitrary.

Fig. 2 shows the tan δ values (the ratio of the storage and loss moduli) of the composites. When its value is higher than one, the sample is considered to behave like a viscous liquid. Correspondingly, a value smaller than one means that the sample behaves more like an elastic solid.

Increased amount of NFC decreases the relative contribution of viscous losses at low angular frequencies as is evident from the values of the tan δ. This is due to nanofibrillated cellulose forming a network of fibrils that are in contact with each other and thus are able to transmit elastic stresses when deformed. Based on our results, the grafted samples appear to be somewhat more elastic signaling of improved contact between the fibrils and the suspending PMMA matrix. With 0.5 wt.% and 1 wt.% of NFC there is still some mobility left in the polymer matrix at low angular frequencies i.e. long characteristic observation times. With 5 wt.% NFC, the sample is gel like, i.e. tan delta is below one, over the complete angular frequency range. The observation that 15 wt.% NFC brings no further advance in the elasticity over the 5 wt.% NFC is likely due to greater degree of aggregation of fibrils with the increased NFC content. This agrees with the visual appearance of the composite plates with 15 wt.% of grafted NFC and also with the complex viscosity values that were lower than expected.

3.2. Mechanical properties

Tensile tests were carried out with composites containing 0.5, 1, and 5 wt.% NFC, since the blends with 15 wt.% NFC content were not processable. The tensile testing results, plotted in Fig. 3, show a slight increase in elastic moduli when the NFC content was 1 wt.% or more. The tensile strength exhibited a decreasing trend from 0 to 1 wt.% of NFC content and increased again slightly at 5 wt.%. Elongation at break was notably decreased from 20% to less than 10% by the addition of even the smallest amount of NFC.

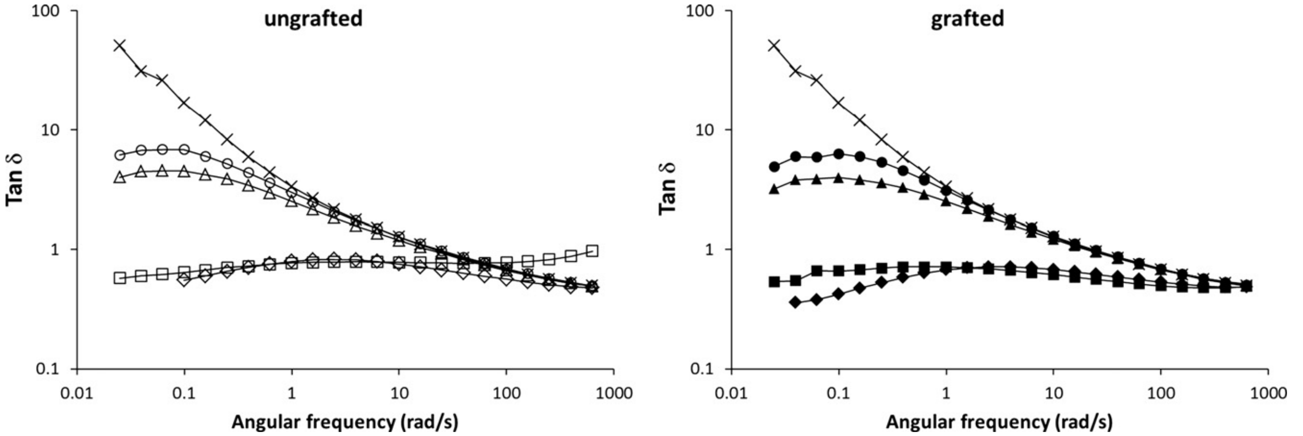

Fig. 2. Tan δ values of PMMA (crosses) and composites with 0.5 wt.% (circles), 1 wt.% (triangles), 5 wt.% (tilted squares), and 15 wt.% (squares) of ungrafted (left) or grafted (right) NFC.

These results indicate that blending with NFC made the composites more rigid but the mechanical strength did not improve even at the highest processable NFC content, despite the percolating nanofiber network. Surprisingly, there was no notable difference between ungrafted and grafted NFC, although the molecular weight of the grafted PMMA was well above the critical molar mass for entanglement coupling (14,000 g/mol) (Fuchs, Friedrich, & Weese, 1996).

3.3. Thermal properties

The glass transition temperatures in Fig. 4, averaged from three measurements, show that the addition of NFC lowered the glass transition temperature of PMMA at all compositions. The measured value for pure PMMA was 107 °C while the values for the composites were between 85 and 100 °C. The glass transition temperature of both composite types had minima at low loadings, after which the T_g values recovered and then decreased more gradually. The minima of grafted and ungrafted NFC were located at 0.5 and 1.0 wt.% compositions, respectively. At load levels up to 1 wt.%, the ungrafted NFC affected T_g more than grafted, whereas on the highest load level the grafted NFC had a more pronounced effect. At 5 wt.%, the difference was within experimental error. Similar behavior of T_g was observed in three measurements.

We compared our results with the literature, since a lowered T_g has also been reported in PMMA/CNC composites (Liu et al., 2010). Unfortunately, CNC concentrations below 2 wt.% were not included in the study but a rapid decrease was observed between 2 and 3 wt.%, after which a plateau was reached. The effect was explained by weakened interactions between polymer chains due to the interpenetrating nanocrystals. However, the presence of hydrogen bonds is generally assumed to raise the glass transition temperature of polymers, and hydrogen bonding functionalities are abundant in both NFC and PMMA (Kuo, 2008). This type of behavior has been reported with electrospun PMMA/CNC fibers that exhibited a higher T_g compared to neat PMMA. After the initial increase, the T_g reached a plateau when the CNC content was above 9 wt.% (Dong et al., 2012). The T_g minima and the lower T_g observed in our study with low content of ungrafted NFC are not explained by this model. The precise values of T_g were not compared due to the different heating rates.

The behavior of T_g suggests that NFC acts as a plasticizer at low concentrations, but this effect considerably weakens at higher concentrations, where the restricting effect of the NFC network also contributes. At low concentrations, the grafted NFC causes less disturbance to the matrix polymer, and therefore the plasticizing effect is not as strong as with the ungrafted NFC. The situation changes at concentrations higher than 5 wt.%. If a continuous nanofibril network is formed, the interactions between the

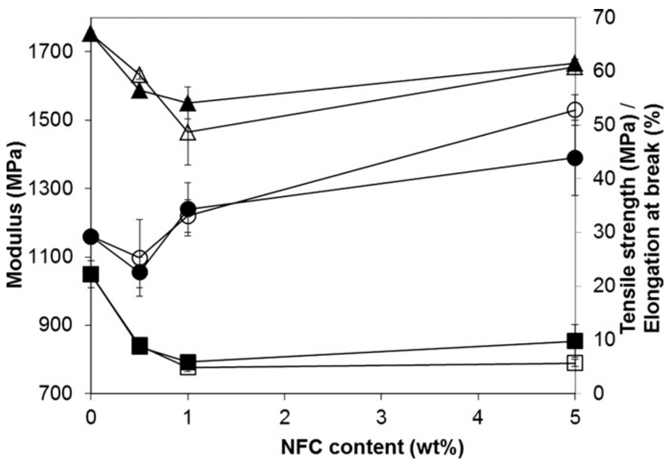

Fig. 3. Elastic modulus (circles), tensile strength (triangles), and elongation at break (squares) of the PMMA/NFC composites with ungrafted NFC (empty symbols) and grafted NFC (filled symbols).

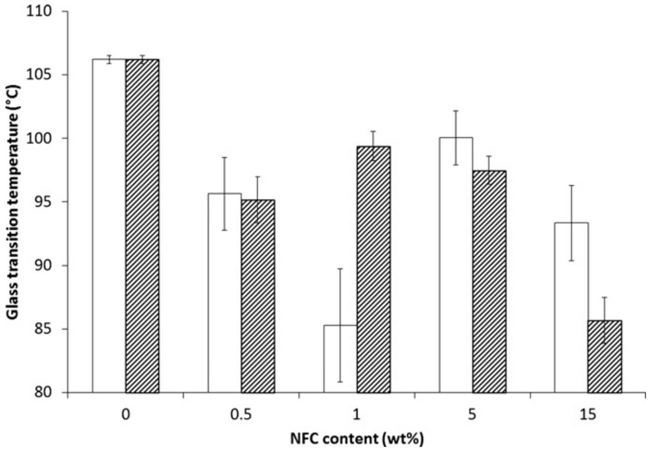

Fig. 4. Glass transition temperatures of PMMA/NFC composites with ungrafted (white columns) and grafted (striped columns) NFC. Standard deviation shown with error bars.

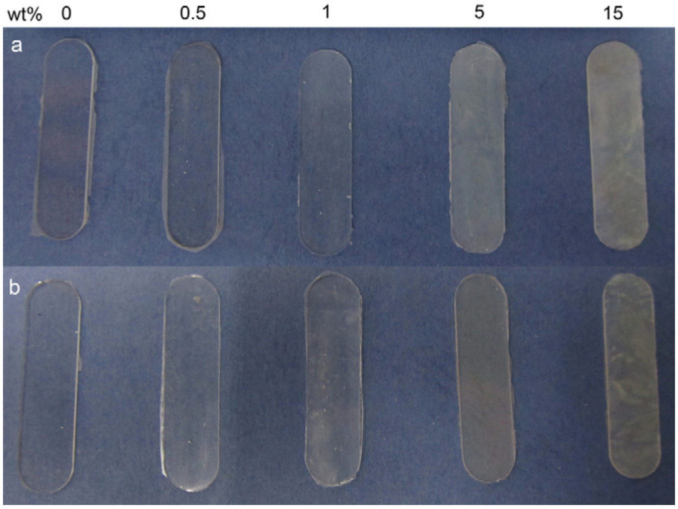

Fig. 5. Compress molded plates (0.5 mm thick) of PMMA reinforced with ungrafted (a) and grafted NFC (b).

nanofibrils are likely weaker in grafted NFC due to the polymer layer covering the fibrils and the possible aggregation during the copolymer synthesis. Therefore, a network of grafted NFC does not limit the chain mobility as effectively as ungrafted NFC.

The observed behavior of T_g is in line with many other studies involving glass transition of nanocomposites. A slightly decreasing T_g has been reported in composites of poly(vinyl alcohol) and microfibrillated cellulose (MFC) with 1–15 wt.% of MFC (Lu, Wang, & Drzal, 2008) and also in PMMA/silica nanocomposites with 0–5 wt.% of silica (Castrillo, Olmos, & González-Benito, 2009). On the other hand, several groups have also reported an increased T_g of composite materials (Cowie, Arrighi, Cameron, McEwan, & McEwen, 2001; Pradhan & Iannacchione, 2010), attributing the decreased mobility of the polymer to strong interactions between the components.

3.4. Optical properties

Optical test specimens are shown in Fig. 5. Increasing opacity can be observed when the weight fraction of both ungrafted and grafted NFC increases. At 5 and 15 wt.% NFC content, some coloration is also evident. The sample with 5 wt.% of grafted NFC was homogeneous in composition, compared to the corresponding sample with ungrafted NFC, but otherwise, there were no notable differences between the different NFC qualities.

The light transmittance values over the visible spectrum, averaged from three measurements, are displayed in Fig. 6. The pure PMMA sample transmitted about 90% of the incident light, and the transmittance was quite constant throughout the studied frequency range. Adding NFC decreased the light transmittance and also skewed the spectrum so that the low wavelengths were affected more than the high. The skewed form of the spectra was similar to an earlier study with CNC/PMMA composites but the light transmittance was less affected by the nanocrystals (Liu et al., 2010). When using unmodified NFC, the transparency gradually decreased as the NFC content increased. The change took place as two large steps at 0.5 and 1.0 wt.% but became much slower at higher weight fractions. However, the behavior of the composites with grafted NFC was more complicated. The transmittance decreased rapidly at 0.5 and 1.0 wt.% and was also slightly lower than with unmodified NFC. At 5 wt.%, the transmittance surprisingly increased and then decreased again. The transmittance of the composites with 5 and 15 wt.% of grafted NFC was also higher than that of the corresponding composites with unmodified NFC.

The stabilization of light transmittance after the steep decrease was possibly caused by the apparent formation of NFC network, which takes place between 1 and 5 wt.%. Below this critical concentration, the nanofibrils are not in contact with each other and there are more transparent regions of pure PMMA that decrease in size when the NFC content increases. Once the nanofibrils start to overlap, increasing their concentration no more significantly affects the optical properties.

The decrease in light transmittance was relatively high at low NFC loadings, compared to PMMA/CNC composites (Liu et al., 2010), although the difference disappeared when at least 5 wt.% of cellulose was added. Cellulose nanofiber reinforced acrylic thermoset composites have been prepared with 60 wt.% cellulose content, with minimal loss of transparency. The difference in optical performance may derive from the finer cellulose nanofibers (bacterial vs. fibrillated) used in the thermoset composites, and the different preparation methods. As the grafting with PMMA was presumed to make NFC more compatible with the polymer, the light transmittance results at low NFC content were unexpected. It should be noted that even though the cellulose content was the same with both NFC types, the grafted variety also contained an equal amount of grafted PMMA. Apparently, this immobilized polymer does not completely blend with the bulk polymer and therefore increases the size of the opaque domains.

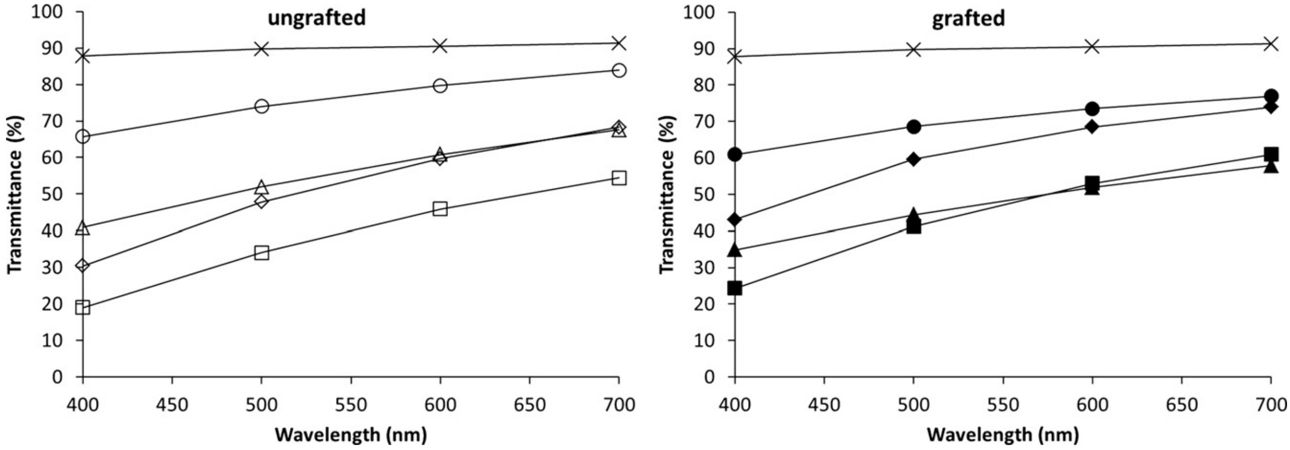

Fig. 6. Visible light transmittance of the compression molded plates of PMMA (crosses) and composites with 0.5 wt.% (circles), 1 wt.% (triangles), 5 wt.% (tilted squares), and 15 wt.% (squares) of ungrafted (left) or grafted (right) NFC.

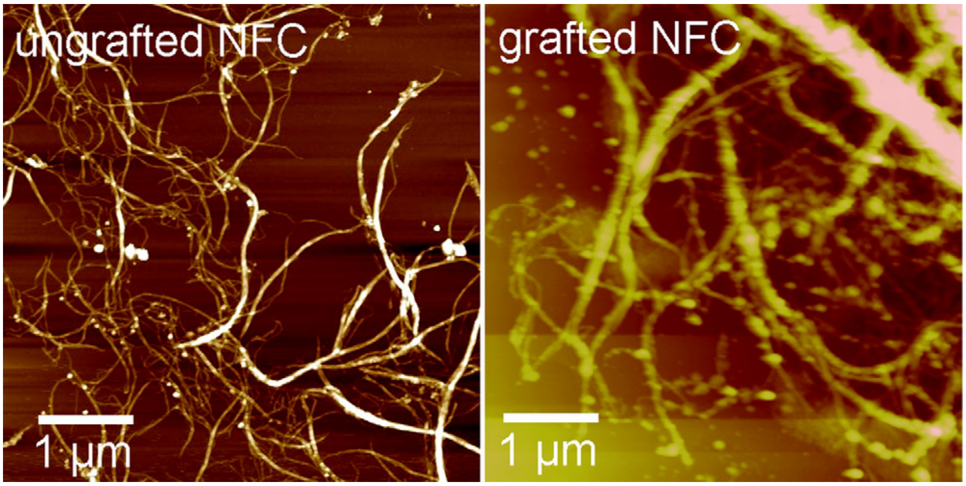

Fig. 7. Topographic AFM images (5 μm × 5 μm) of unmodified (left, from Littunen et al., 2011) and grafted NFC.

3.5. Microscopic imaging

Microscopic images of unmodified and grafted NFC obtained by AFM are shown in Fig. 7. The image of unmodified NFC shows an entangled network of separate fibrils between 30 and 80 nm in diameter. After grafting, the fibril diameter was increased to approximately 70–200 nm. The increased size of the fibrils was probably caused by the addition of grafted polymer that is shown in the image as small globules attached on the surface of the fibrils. The fine structure of NFC was relatively well preserved, although some level of aggregation was evident due to a number of large fibril bundles observed among the smaller fibrils. A probable reason for the aggregation was the screening of the negative surface charge of NFC caused by the polymer coating, decreasing the repulsive electrostatic interfibrillar forces.

In order to get information about the composite microstructure and the dispersion of NFC, SEM images of some composites were taken. Samples with 1 and 5 wt.% of NFC were selected for imaging, since the percolation threshold of NFC was indicated to be between these compositions. The composites appeared similar at small magnifications (1000×). However, differences became visible at higher magnifications. The micrographs of the fracture surfaces at 10,000× magnification are shown in Fig. 8. The composite with 1 wt.% NFC had some rough regions, apparently covered by a nanofiber mesh, among smoother domains of neat PMMA. At 5 wt.% NFC content, the mesh-like texture was present throughout the fracture surface, thus confirming the presence of a percolating network that was indicated by rheological properties. There was no visible difference between samples with ungrafted or grafted NFC.

3.6. Molar mass

Molar masses of the PMMA phase of the composites were measured after injection molding to detect possible degradation of the PMMA matrix caused by melt processing. The data presented in Table 1 shows that the number average molar mass and the PDI were not significantly affected by the presence of NFC during the melt processing. There was virtually no polymer degradation in the composites of grafted NFC. The composites with ungrafted NFC exhibited a small but consistent decrease of molar mass and also slightly higher PDI. These results suggest the presence of some residual moisture in ungrafted NFC, which can be detrimental to PMMA at elevated temperatures. The layer of grafted polymer on the nanofibrils apparently prevents this type of degradation either by promoting the drying of NFC or by obstructing the direct contact between NFC and PMMA.

3.7. Discussion of the combined results

To summarize the experimental results, there was a leap in melt viscosity of the composites with 1–5 wt.% of NFC, accompanied by a transition of the material into gel state. Light transmittance decreased rapidly from 0 to 1 wt.%, leveling off at higher NFC loadings. T_g also decreased in the same concentration range, having minima at 0.5 wt.% of grafted NFC, and 1 wt.% of ungrafted NFC. The molar mass of the matrix polymer was unaffected by the NFC content and therefore did not explain these results.

Based on the thermal, rheological, and optical properties, a fundamental change takes place when the NFC content is increased from 1 to 5 wt.%. Since the tan δ values indicate a transition from liquid to gel in molten state, the formation of a percolating NFC network is likely somewhere between 1 and 5 wt.% NFC content. This assumption was also confirmed by SEM images. For comparison, gel formation in aqueous suspensions has been observed already at 0.125 wt.% of NFC (Pääkkö et al., 2007). The difference is caused by the weaker interaction between the polymer and NFC. The NFC concentration required for gel formation is dependent on the conformation of the nanofibrils, which is more extended in a very polar medium, like water, and becomes contracted in less polar media, like THF and PMMA. Extended nanofibrils occupy more space than contracted nanofibrils and therefore also become entangled at a lower concentration.

The continuous network may be more stable than separated nanofibrils during the solvent evaporation, preventing the formation of aggregates. At 0.5–1 wt.%, the nanofibril suspension is too

Table 1
Molar masses of PMMA and PMMA/NFC composites after injection molding.

NFC type	NFC content (wt.%)	M_n (g/mol)[a]	PDI[a]
None	0	63,100	1.71
Ungrafted	0.5	57,800	1.84
	1	58,800	1.86
	5	58,200	1.82
	15	58,100	1.98
Grafted	0.5	61,400	1.73
	1	62,700	1.76
	5	65,400	1.71
	15	64,100	1.71

[a] Measured by GPC.

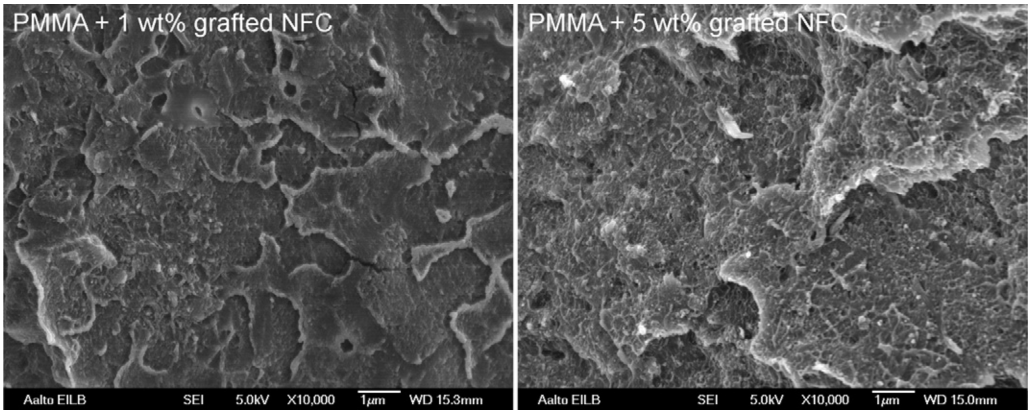

Fig. 8. SEM images taken at 10,000× magnification of PMMA composites with 1 wt.% (left) and 5 wt.% (right) of grafted NFC.

dilute for any fibril entanglement to occur and especially ungrafted fibrils are in small separated bundles. When the solvent is removed, these bundles collapse and form aggregates. This would explain the rapid decrease of T_g and light transmittance at these NFC loadings, as the aggregates induce both the increasing opacity, and the plasticizing effect discussed in Section 3.3. At 5 wt.% however, there is a continuous network structure that is kept intact by entanglements, preserving similar network structure in the polymer matrix. Since further increase of NFC loading from 5 to 15 wt.% has only minor effect on the composite properties, there are apparently no more significant changes in the density of NFC network. In fact, the rheological data suggests that the network becomes oversaturated at the highest NFC loading and the excess NFC is separated from the bulk composite as aggregates.

4. Conclusion

Melt processable composites of PMMA and NFC were prepared by blending ungrafted and grafted NFC with the dissolved polymer and evaporating the solvent. Injection and compression molded test specimen were prepared and analyzed for molar mass, microstructure, and for mechanical, rheological, thermal, and optical properties.

Formation of a percolating network somewhere in between 1 and 5 wt.% was indicated by rheological behavior, and the nanofiber network was also visible in SEM images. The critical NFC content for percolation was significantly higher than the one reported for water suspensions due to the weaker interaction between the nanofibrils and the surrounding medium.

The behavior of glass transition temperature suggested a plasticizing effect of especially unmodified NFC at low concentrations, indicating weak interaction with the matrix polymer. At higher NFC content, the movement of PMMA chains became more restricted due to the percolating NFC network.

Unmodified NFC was found to cause slight degradation of the matrix polymer during the melt processing. The fibrillar fine structure of NFC was well preserved after grafting, and the attached polymer layer apparently protected the matrix polymer from the degradation by preventing its direct contact with the residual moisture in NFC. The addition of NFC improved the mechanical properties of PMMA slightly. However, the transparency of the composites was notably decreased already at the lowest NFC content.

The results of the study suggest that the preparation of composites of NFC and hydrophobic thermoplastics remains a very challenging task. In addition to the percolating nanofibril network, improved interfacial adhesion is also required to benefit from the mechanical properties of NFC. Surprisingly, the adhesion was unaffected by the polymer grafting of NFC. The apparent lack of entanglements and the visible heterogeneity of the composites suggested an insufficient mixing of the components during the solution blending. Improved results may be obtained by utilizing more efficient mechanical stirrers.

Acknowledgments

This work has been carried out as part of the project “Tailoring of nanocellulose structures for industrial applications (NASEVA)”, funded by the Finnish Funding Agency for Technology and Innovation (TEKES). UPM Corporation is acknowledged for supplying the UPM Fibril Cellulose raw material. The authors would also like to thank Minna Annala for helpful discussions, Dr. Vesa Vuorinen for the SEM imaging, and Dr. Justin Zoppe for the AFM imaging.

References

Berglund, L. (2005). Cellulose-based nanocomposites. In A. K. Mohanty, M. Misra, & L. T. Drzal (Eds.), *Natural fibers, biopolymers and biocomposites* (pp. 807–832). Boca Raton: Taylor & Francis Group.

Bondeson, D., & Oksman, K. (2007). Polylactic acid/cellulose whisker nanocomposites modified by polyvinyl alcohol. *Composites Part A: Applied Science and Manufacturing*, *38*(12), 2486–2492.

Canché-Escamilla, G., Rodriguez-Laviada, J., Cauich-Cupul, J. I., Mendizábal, E., Puig, J. E., & Herrera-Franco, P. J. (2002). Flexural, impact and compressive properties of a rigid-thermoplastic matrix/cellulose fiber reinforced composites. *Composites Part A: Applied Science and Manufacturing*, *33*(4), 539–549.

Castrillo, P. D., Olmos, D., & González-Benito, J. (2009). Novel polymer composites based on a mixture of preformed nanosilica-filled poly(methyl methacrylate) particles and a diepoxy/diamine thermoset system. *Journal of Applied Polymer Science*, *111*(4), 2062–2070.

Cowie, J. M. G., Arrighi, V., Cameron, J., McEwan, I., & McEwen, I. J. (2001). Lyotropic liquid crystalline cellulose derivatives in blends and molecular composites. *Polymer*, *42*(24), 9657–9663.

Dong, H., Strawhecker, K. E., Snyder, J. F., Orlicki, J. A., Reiner, R. S., & Rudie, A. W. (2012). Cellulose nanocrystals as a reinforcing material for electrospun poly(methyl methacrylate) fibers: Formation, properties and nanomechanical characterization. *Carbohydrate Polymers*, *87*(4), 2488–2495.

Fuchs, K., Friedrich, C., & Weese, J. (1996). Viscoelastic properties of narrow-distribution poly(methyl methacrylates). *Macromolecules*, *29*(18), 5893–5901.

Helbert, W., Cavaillé, J. Y., & Dufresne, A. (1996). Thermoplastic nanocomposites filled with wheat straw cellulose whiskers. Part I: Processing and mechanical behavior. *Polymer Composites*, *17*(4), 604–611.

Isobe, N., Sekine, M., Kimura, S., Wada, M., & Kuga, S. (2011). Anomalous reinforcing effects in cellulose gel-based polymeric nanocomposites. *Cellulose*, *18*(2), 327–333.

Kuo, S. (2008). Hydrogen-bonding in polymer blends. *Journal of Polymer Research*, *15*(6), 459–486.

Littunen, K., Hippi, U., Johansson, L., Österberg, M., Tammelin, T., Laine, J., et al. (2011). Free radical graft copolymerization of nanofibrillated cellulose with acrylic monomers. *Carbohydrate Polymers*, *84*, 1039–1047.

Liu, H., Liu, D., Yao, F., & Wu, Q. (2010). Fabrication and properties of transparent polymethylmethacrylate/cellulose nanocrystals composites. *Bioresource Technology*, *101*(14), 5685–5692.

Lu, J., Wang, T., & Drzal, L. T. (2008). Preparation and properties of microfibrillated cellulose polyvinyl alcohol composite materials. *Composites Part A: Applied Science and Manufacturing*, *39*(5), 738–746.

Nakagaito, A. N., & Yano, H. (2005). Novel high-strength biocomposites based on microfibrillated cellulose having nano-order-unit web-like network structure. *Applied Physics A: Materials Science and Processing*, *80*(1), 155–159.

Nogi, M., Handa, K., Nakagaito, A. N., & Yano, H. (2005). Optically transparent bionanofiber composites with low sensitivity to refractive index of the polymer matrix. *Applied Physics Letters*, *87*(24), 243110.

Nordgren, N., Lonnberg, H., Hult, A., Malmstrom, E., & Rutland, M. W. (2009). Adhesion dynamics for cellulose nanocomposites. *ACS Applied Materials & Interfaces*, *1*(10), 2098–2103.

Pääkkö, M., Ankerfors, M., Kosonen, H., Nykänen, A., Ahola, S., Österberg, M., et al. (2007). Enzymatic hydrolysis combined with mechanical shearing and high-pressure homogenization for nanoscale cellulose fibrils and strong gels. *Biomacromolecules*, *8*(6), 1934–1941.

Pradhan, N. R., & Iannacchione, G. S. (2010). Thermal properties and glass transition in PMMA + SWCNT composites. *Journal of Physics D: Applied Physics*, *43*(30), 305403.

Taubner, V., & Shishoo, R. (2001). Influence of processing parameters on the degradation of poly(L-lactide) during extrusion. *Journal of Applied Polymer Science*, *79*(12), 2128–2135.

Turbak, A. F., Snyder, F. W., & Sandberg, K. R. (1983). Nanofibrillated cellulose, a new cellulose product: Properties, uses, and commercial potential. *Journal of Applied Polymer Science: Applied Polymer Symposium*, *37*, 815–827.